RSC Advances

PAPER

View Article Online
View Journal | View Issue

Cite this: *RSC Adv.*, 2020, **10**, 3520

Molecular modelling and synthesis of a new collector *O*-butyl *S*-(1-chloroethyl) carbonodithioate for copper sulfide ore and its flotation behavior

Xiaopeng Chi, *[abc] Yunshan Guo,[abc] Shuiping Zhong,[a] Guoyao Li[a] and Xulong Lv[d]

Received 26th November 2019
Accepted 2nd January 2020

DOI: 10.1039/c9ra09648e

rsc.li/rsc-advances

Based on the homology principle in advanced pharmaceutical chemistry, a new high efficiency and low toxicity collector, *O*-butyl *S*-(1-chloroethyl)carbonodithioate, was designed. By using molecular simulation technology, MS (Materials Studio) was used to build the molecular model of the collector. The molecular structure was relaxed and optimized. The process of interaction between reagent and mineral surface was simulated and the interaction energy of reagent and mineral surface was calculated by density functional theory (DFT). The interaction process of the new collector and butyl xanthate on the mineral surface and the interaction energy of these two reagents and mineral surface were compared. The molecular structure of the new collector was designed from the perspective of the difference of the interaction energy between the reagents and the mineral surface. According to the results of molecular design and modelling, the new collector was synthesized. The flotation tests of pure minerals and real ores were carried out to verify the new collector. The experimental results showed that the collector has the characteristics of low toxicity, high selectivity, moderate collecting ability and low cost, and it is more suitable for flotation of the complex and refractory copper sulfide with low grade and fine dissemination.

1. Introduction

With the continuous exploitation of mineral resources, sulfide ores gradually become low grade, and have a fine grain and complicated composition. Xanthate, as the most widely applicable sulfide collector, needs to be used in combination with butyl dithiophosphate,[1] polyglutamic acid[2] or other regulators to achieve better separation. Therefore, more and more new collectors have been researched and developed. With the emergence of computer-aided means, the situation of screening new collectors only by experiments has been changed, and the research efficiency of flotation reagents has been greatly improved. In 1970, Glembotsky[3] pointed out the existence of characteristic functional groups in organic reagents in the article "search and design of flotation reagents with known properties", and the mechanism of these characteristic functional groups can be used as the basis for molecular design of new flotation reagents. In 1980, Ariens[4] also studied the application of a "drug design" method in the study of new flotation reagents in the work of "drug design". Jian[5] applied six principles in advanced pharmaceutical chemistry: homology principle, vinylogy principle, isosterism principle, isomerism principle, analogs principle and hybridization principle to the molecular design and research of flotation reagents. In recent years, Wang *et al.*[6] developed the molecular design of flotation reagents to the stage of quantitative design on the basis of previous studies on the relationship between the structure and performance of flotation reagents. Based on GPT equation, the relationship between energy criterion and group electronegativity, compound concentration product and flotation activity was studied by Jiang *et al.*[7]

Recently, on the basis of the improvement of molecular design theory for flotation reagents, computer-aided molecular design has been widely used in the design, simulation and synthesis of new flotation reagents. Mohamed. *et al.*[8] solved the hydrophobicity of the main negative ions in soaps by using the adsorption locator module in MS (Materials Studio). Jain *et al.*[9] used MS to construct the initial structure of ligands and complexes, and used DFT (density functional theory) to calculate the interactions of salicylaldoxime (SALO) and its derivatives possessing appropriate alkyl group substitution in the main chain(CM-SALO) or side chain (CS-SALO) with copper, zinc and lead divalent ions, so as to understand the interaction mechanism. Liu *et al.*[10] used Gaussian03 and Chemoffice2005 to build a molecular model and DFT to study the structural

[a]*State Key Laboratory of Comprehensive Utilization of Low-Grade Refractory Gold Ores, Zijin Mining Group Co.,Ltd., Shanghang, 364200, China. E-mail: xiaopengchi@fzu.edu.cn*

[b]*School of Zijin Mining, Fuzhou University, Fuzhou, Fujian, 350108, China*

[c]*Fuzhou University-Zijin Mining Group Joint Research Center for Comprehensive Utilization of Mineral Resources, Fuzhou, Fujian, 350108, China*

[d]*Zijin Copper Industry Co., Ltd., Shanghang, Fujian, 364000, China*

response of sulfur phosphorus molecule with sulfide ores. Otero-Calvi *et al.*[11] used PyMOlyze (the program PyMOlyze) to analyze molecular orbital, and DFT to study the main types of interaction between metals and ligands.

According to the homology principle[12] in advanced pharmaceutical chemicals,[12] a new collector for sulfide ore, *O*-butyl *S*-(1-chloroethyl)carbonodithioate, with low cost, high selectivity, moderate collecting ability and low toxicity was designed. By using molecular simulation technology, MS (Materials Studio) was used to build the molecular model of collector. The molecular structure was then optimized in the way of relaxation and introversion to obtain the mineral surface with the lowest surface energy. And the lowest energy configuration of the interaction between the reagents and mineral surfaces was obtained by dynamic simulation of reagent molecules and mineral surfaces. The interaction energy of the reagents and mineral surfaces was calculated by DFT (density functional theory). According to the interaction energy between the reagents and the mineral surfaces and the dynamic simulation results, the new collector for sulfide ore was designed and synthesized. The new collector, *O*-butyl *S*-(1-chloroethyl)carbonodithioate, was then verified by the flotation test of pure minerals and read ores, which proved that it has a better separation effect on the complex and refractory copper sulfide ores with low grade and fine dissemination.

2. Materials and methods

2.1 Materials and reagents

The test samples were from a chalcopyrite mine in Guizhou province and a pyrite mine in Guilin, Guangxi province. The monominerals with 98% purity were obtained by hand sorting after grinding of raw ore. The actual ore were form Duobaoshan copper molybdenum mine in Heilongjiang province, in which the copper minerals were mainly chalcopyrite, followed by chalcocite and bornite, and gangue minerals were mainly pyrite and quartz. The multi-element analysis results of the actual ore were shown in Table 1. And its XRD (DY5261/Xpert3, CEM company, USA) diagrams were shown in Fig. 1 and 2.

The chemical reagents used in this study included: analytical-grade sodium hydroxide (NaOH, Xilong Chemical Co., Ltd., Guangdong, China) and analytical-grade hydrochloric acid (HCl, Xilong Chemical Co., Ltd., Guangdong, China) for pH adjustment; analytical-grade butyl xanthate as the collector. The new reagent was synthesized from analytical pure chemical reagents. According to the homology principle[12] in advanced pharmaceutical chemicals,[12] the physical properties and chemical reactions of homologues are all changed in the same way, a new collector for sulfide ore, GC-I (*O*-butyl *S*-(1-chloroethyl)carbonodithioate), was synthesized by butyl xanthate and 1,1-dichloroethane and its chemical structure formula as follows:

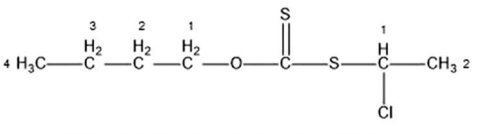

O-butyl *S*-(1-chloroethyl) carbonodithioate

In order to further analyze its chemical properties, the new reagent GC-I was analyzed by infrared spectroscopy. The infrared spectroscopy analysis results of GC-I were shown in Fig. 3.

As shown in Fig. 3: GC-I is a kind of lipid collector. CH_3 symmetrical bending vibration absorption peak and asymmetric bending vibration absorption peak are at 1367.6 cm^{-1} and 1463.3 cm^{-1} respectively, and CH_2 symmetrical bending

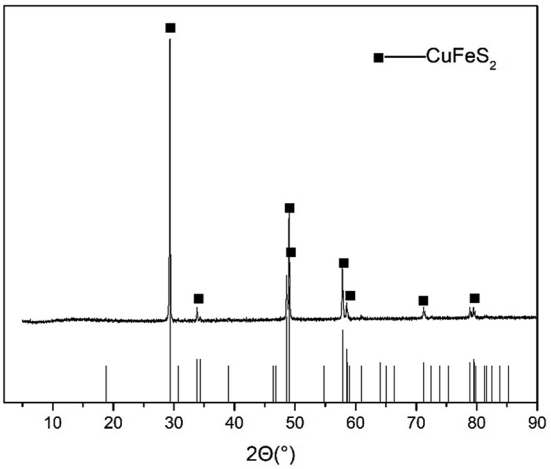

Fig. 1 X-ray diffraction analysis of chalcopyrite.

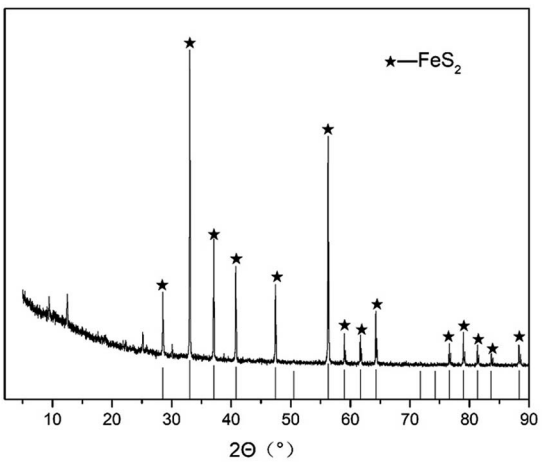

Fig. 2 X-ray diffraction analysis of pyrite.

Table 1 Multi-element analysis results of actual ore (mass fraction)/%

Component	Cu	Pb	Zn	S	Mo	Au[a]	Ag[a]
Content	0.43	0.004	0.039	0.68	0.009	0.01	2.8
Component	Fe	Ca	Mg	SiO_2	Al	P	As
Content	5.83	3.01	1.22	67.32	7.31	0.01	0.001

[a] Au, Ag unit g t^{-1}.

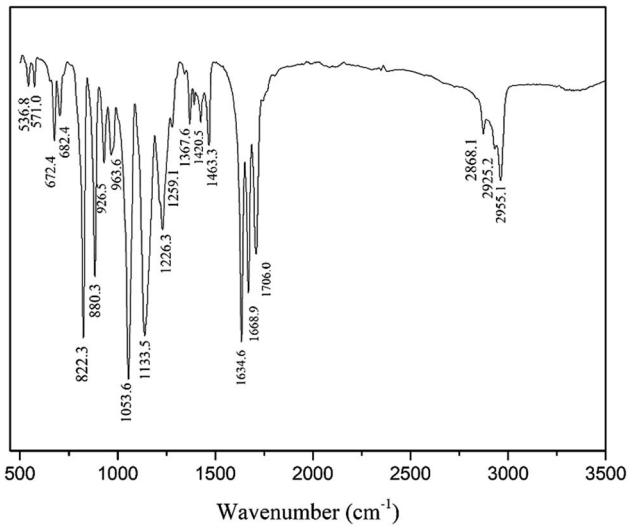

Fig. 3 The IR spectrum of GC-I.

vibration absorption peak and asymmetric bending vibration absorption peak are at 2868.1 cm^{-1} and 2955.1 cm^{-1} respectively. There are C–O–C asymmetric stretching vibration absorption peak at 1133.5 cm^{-1} and 1226.3 cm^{-1}. There is a stretching vibration absorption peak of C–Cl bond at 682.4 cm^{-1} and an asymmetric stretching vibration absorption peak at 1053.6 cm^{-1}.

2.2 Molecular dynamics simulation

The calculations were performed in the framework of the MD, using the Material Studio (MS) package. By consulting the crystal database ICSD, the cell parameters and atomic coordinates of each mineral were obtained. Using the Cambridge Sequential Total Energy Package (CASTEP) module of MS, the crystal structure of chalcopyrite and pyrite was optimized from two aspects of "band structure" and "density of states" respectively. In order to obtain better optimization effect in the structural optimization, the relative error before and after crystal parameters optimization should be within 0–2% under the condition of energy convergence in the optimization process. The optimization parameters were as follows: a function was modified with Perdew–Burke–Ernzerhof generalized gradient approximation (PBEsol GGA); the *k*-point set of chalcopyrite and pyrite was 5 × 5 × 2 and 4 × 4 × 2; the self-consistent-field (SCF) tolerance was 1.0×10^{-6} eV per atom; and the custom energy cut-off of chalcopyrite and pyrite was 400 eV and 353.7 eV. Other parameters were default values. The lattice optimization results were shown in Table 2. Then, 2D periodic surface cells were created from the unit cells of chalcopyrite[13–15] and pyrite[16] at the cleavage plane (101)and (101), respectively. The optimized chalcopyrite surface slab was extended to a periodic super lattice of approximately 25 Å × 20 Å with a certain vacuum thickness of 27 Å. The optimized pyrite surface slab was extended to a periodic super lattice of

Table 2 Cell parameters of chalcopyrite and pyrite

Minerals	Crystal	Space group	Cell parameters	DFT predicted cell parameters
Chalcopyrite	Tetragonal	$I\bar{4}2d$	$a_0 = b_0 = 0.52$ nm $c_0 = 1.03$ nm, $z = 4$	$a_0 = b_0 = 0.51$ nm $c_0 = 1.01$ nm, $z = 4$
Pyrite	Cubic	*Pa*3	$a_0 = b_0 = c_0 = 0.54$ nm $z = 4$	$a_0 = b_0 = c_0 = 0.54$ nm $z = 4$

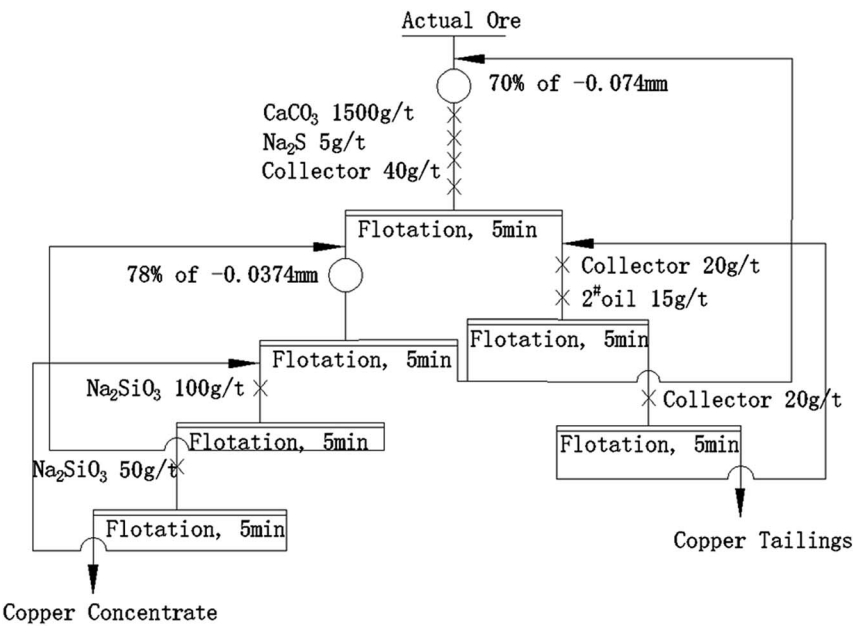

Fig. 4 Closed-circuit flotation flowsheet of actual ores.

approximately 37 Å × 43 Å with a certain vacuum thickness of 24 Å.[17] After reconstruction and optimization, copper ion on the surface of chalcopyrite was optimized from the first layer to the second layer, and sulfur ion of pyrite was optimized from the second layer to the first layer.

The optimization molecular modelling of GC-I (*O*-butyl *S*-(1-chloroethyl)carbonodithioate) and butyl xanthate was obtained by using "CASTEP" and "Forcite" of MS (Materials Studio). The geometry optimization of the system of reagent-mineral was conducted using the "Forcite" of MS, and the atom-based cut-off method was employed for calculating both the van der Waals and electrostatic interactions (coulombic).[17] The atom-based cut-offs were used with a 15.5 Å cut-off distance, with a spline width of 1.0 Å and a buffer width of 0.5 Å.

The coordinates of surface atoms were constrained during the MD simulations with the adsorbates being free. All simulations were performed at constant volume and temperature (NVT).The interaction energy between the reagent and minerals were calculated according to the following formula[18,19]:

$$E_i = E_t - (E_m + E_r)$$

E_i—negative magnitudes of interaction energy; E_t—energy of the optimized reagent-mineral complex; E_m—energy of surface cluster; E_r—energy of reagent molecule.

2.3 Flotation experiments

The flotation test of monominerals was carried out in XFGC II hanging trough flotation machine. Monominerals manually selected with 2.0 g each time were added to the flotation tank after ultrasonic cleaning. Then distilled water 45 mL was added to, mixed 3 min. The pulp pH was adjusted by HCl and NaOH. After stirring 2 min, the collector and frother were added in turn. The flotation time was 6 minutes, and the speed of flotation machine was 1600 rpm. The flotation test for actual ore was carried out in XFG-3L flotation cell. The amount of ore samples in each experiment was 1000*g*. The concentrates and tailings obtained by flotation test were dried, weighed and element content analyzed, and the grade and recovery were calculated. The closed-circuit flotation flowsheet was shown in Fig. 4.

2.4 FTIR measurements

The infrared spectrum was made by AVATAR360 intelligent Fourier Transform Infrared Spectrometer (AVATAR360 intelligent, produced by Nikoli instrument company, USA). The ore sample was ground to 5 μm and was added into a suitable amount of collector solution. After stirring for 30 minutes, the ore sample was filtered out and washed with distilled water three times. And then, the obtained solid was dried in a vacuum oven at 40 °C for 12 h, the test samples were obtained finally. It is necessary to ensure that samples are not contaminated throughout the process. The 5 mg sample was mixed with 500 mg dried KBr and pressed into thin slices with a diameter of 1 cm. Then the infrared spectrum was measured.

2.5 Adsorption measurements

Firstly, the shading degree of different concentration of GC-I was measured, and the corresponding curve of GC-I concentration and shading degree was drawn according to the data. The ore sample with 2 g was put into beaker and 100 mL distilled water added into the beaker to mix. The slurry pH was then adjusted to 7 by using pH regulators. After adsorption, the pulp is centrifugally separated. After standing, the supernatant was taken to measure the shading degree. The concentration of GC-I in the solution was calculated according to the known standard curve. The adsorptive quantity of the reagent was calculated according to the following formula.[20] The specific surface area of chalcopyrite was 1.93 $m^2\ g^{-1}$ and that of pyrite was 1.045 $m^2\ g^{-1}$, which were measured by BET nitrogen adsorption method.

$$\Gamma = \frac{V(C_0 - C)}{mA}$$

Γ—Adsorptive quantity of collector on mineral surface, C_0—concentration of collector in supernatant, C—concentration of added collector, V—volume of the solution, m—mass of the sample, A—Specific surface area of the ore particles.

3. Results and discussion

3.1 Computation of interaction energy by MD simulations

MD simulations were used to describe the crystal structure specificity of collector molecules with different minerals. The computed interaction energies of GC-I (*O*-butyl *S*-(1-chloroethyl) carbonodithioate) and butyl xanthate molecules with chalcopyrite (101) and pyrite (101) were compared in Table 3, and the final adsorption configurations of collector with minerals were shown in Fig. 5.

As illustrated in Table 3, the interaction energy between GC-I and chalcopyrite was −846.89 kJ mol^{-1}, while the interaction energy between butyl xanthate and chalcopyrite was −615.49 kJ mol^{-1}. This indicates that GC-I was more likely to interact with chalcopyrite than butyl xanthate; the interaction energy between GC-I and pyrite was −46.19 kJ mol^{-1}, while the interaction energy between butyl xanthate and pyrite was −60.24 kJ mol^{-1}, which proved that the interaction energy between GC-I and pyrite was more difficult. Therefore, butyl xanthate was more likely to interact with pyrite than GC-I.

3.2 Monomineral flotation

3.2.1 Effects of pH value on flotation behaviour. In order to investigate the collection performance of GC-I and butyl xanthate for chalcopyrite and pyrite under different pH, the

Table 3 Interaction energy calculation results/kJ mol^{-1}

Name	E_i
Chalcopyrite + GC-I	−846.89
Chalcopyrite + butyl xanthate	−615.49
Pyrite + GC-I	−46.19
Pyrite + butyl xanthate	−60.24

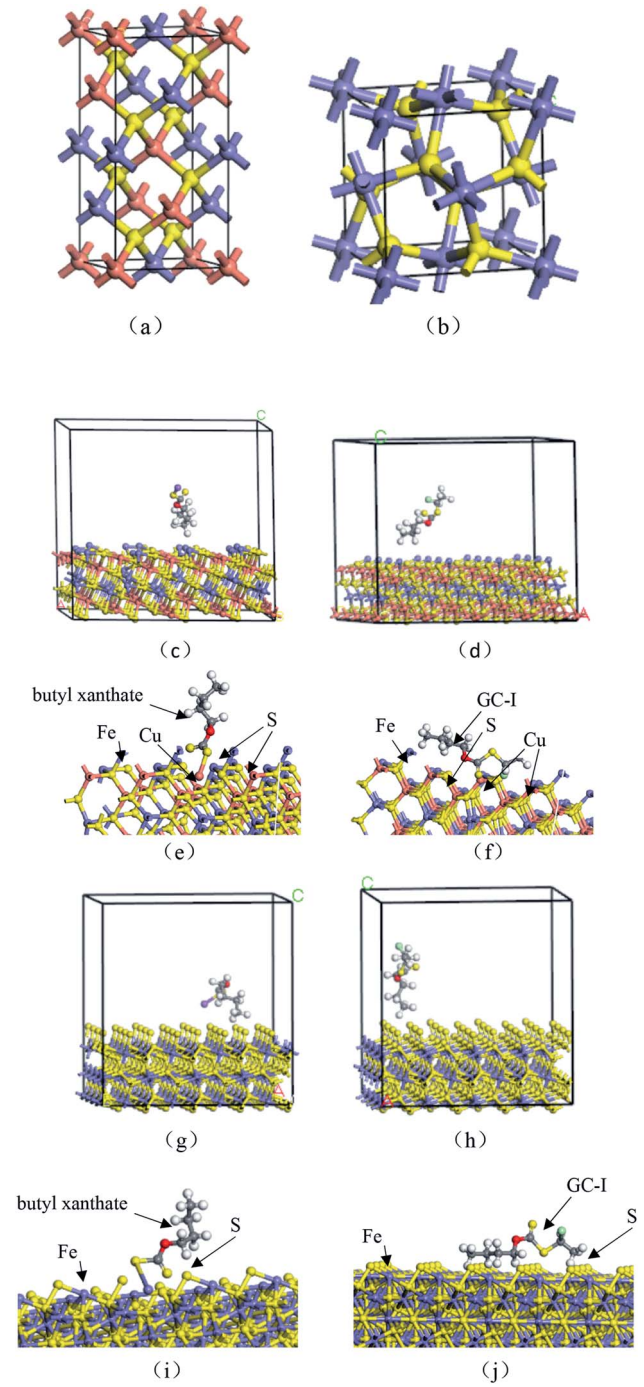

Fig. 5 Interaction model of reagents and minerals: (a) crystal structure model of chalcopyrite; (b) crystal structure model of pyrite; (c) crystal model of interaction between butyl xanthate and chalcopyrite; (d) crystal model of interaction between GC-I and chalcopyrite; (e) butyl xanthate on chalcopyrite surface; (f) GC-I on chalcopyrite surface; (g) crystal model of interaction between butyl xanthate and pyrite; (h) crystal model of interaction between GC-I and pyrite; (i) butyl xanthate on pyrite surface; (j) GC-I on pyrite surface.

comparative experiments of chalcopyrite monomineral and pyrite monomineral as raw material were conducted. In the process of mineral flotation, pH will affect the electrical properties of particles surface,[21] the hydrolysis of cations on particles

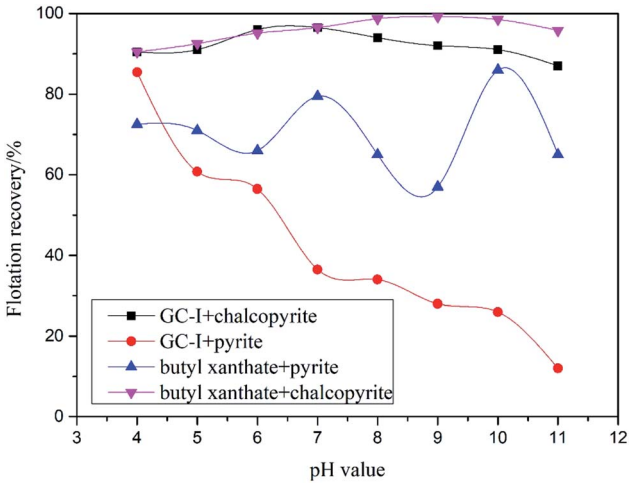

Fig. 6 Effect of pH value on recovery of chalcopyrite and pyrite using different reagents.

surface, the hydrolysis of collectors, the adsorption of collectors at solid–liquid interface and the flotability of materials.[22] As it is widely known, CaO had a strong inhibition effect on the flotation of pyrite[23] and the Ca^{2+} generated will inhibit chalcopyrite flotation at a certain concentration.[24] Therefore, HCl and NaOH were used as regulators to adjust the pH of the ore pulp, so that the flotation environment can be stabilized within the appropriate pH range and the performance of collectors will be fully utilized. The experiment was performed in a 160 mg L^{-1} of collector and a 5 mg L^{-1} of $2^{\#}$oil. HCl and NaOH were used as regulators to adjust the pH of the ore pulp. The results were shown in Fig. 6.

As shown in Fig. 6, the pH had little effect on the collection performance of chalcopyrite and the recoveries of several collectors were over 87%. However, the collection effect of GC-I on pyrite gradually decreased with the increase of pH. When the pH increased to 11, the recovery of pyrite decreased to 12%. The

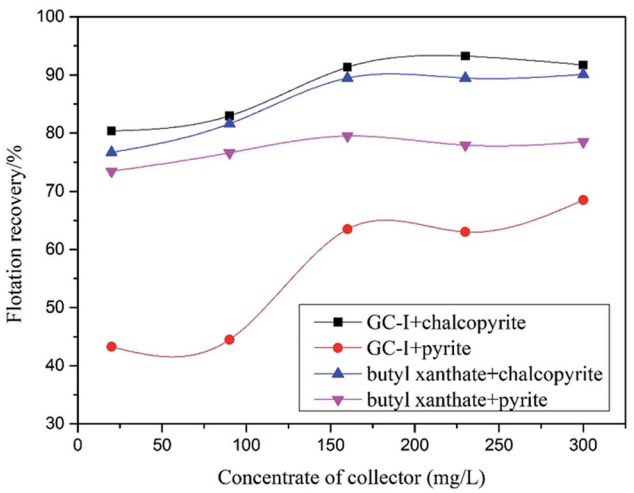

Fig. 7 Effect of dosage of reagent on recovery of chalcopyrite and pyrite using different reagents.

pulp nature pH value is pH 7. The collecting performance of GC-I on chalcopyrite was the same as that of butyl xanthate at pH 7. Compared with butyl xanthate, GC-I had stronger selectivity at pH 7. The recoveries of chalcopyrite and pyrite by GC-I as collector were 96.5% and 36.5% respectively at pH 7. It showed that copper–sulphur separation was realized, and better flotation indexes were obtained by using GC-I as collector.

3.2.2 Effects of collector dosage on flotation behavior. The comparative experiments of collector type and dosage were conducted at pH 7. The results were shown in Fig. 7.

As can be seen from Fig. 7, the flotation of chalcopyrite and pyrite by butyl xanthate and GC-I reached a dynamic balance with the increase of collector dosage. When the dosage of collector was 160 mg L^{-1}, the recovery of chalcopyrite and pyrite by butyl xanthate were 89.5% and 79.5%, and the recovery of chalcopyrite and pyrite by GC-I were 96.5% and 63.5%. It showed that the flotation performance of GC-I was the best.

3.3 Closed circuit flotation of actual ores by GC-I

In order to further verify the flotation effect of GC-I on actual ore, the flotation comparison tests of actual ores from Duobaoshan were carried out. In view of the actual copper ores from Duobaoshan, a closed-circuit flotation process with once roughing, twice scavenging, roughing concentrate regrinding, three times cleaning for regrind concentrate was adopted. A comparative flotation tests between butyl xanthate and the new reagent GC-I were carried out with the same reagent system. The flotation test flowsheet was shown in Fig. 4. The test results were shown in Table 4.

From Table 4, aiming at Duobaoshan actual copper ore, under the closed circuit test process of with once rough separation, twice scavenging, roughing concentrate regrinding, three times cleaning for regrind concentrate and under the same dosage of reagent, the grade of copper concentrate obtained by using GC-I as collector was 17.14% higher than that obtained by using butyl xanthate as collector. At the same time, the recovery rates were basically the same.

3.4 FTIR analysis results

The corresponding chelates were formed by the interaction between collector mainly through the organo-functional groups and corresponding metal ions. Because of its hydrophobicity, chelates combined with bubbles in the pulp and floated to the pulp level, thus realizing the flotation separation of minerals. Therefore, detecting the functional groups of GC-I interacting with minerals and exploring the interaction modes between GC-I and mineral surfaces were the keys of the GC-I mechanism analysis.

Table 4 Results of closed circuit flotation for actual ores/%

	Productivity		Copper grade		Copper recovery	
Products	IBX	GC-I	IBX	GC-I	IBX	GC-I
Concentrate	1.50	0.82	19.88	37.02	80.74	80.70
Tailings	98.50	99.18	0.072	0.073	19.26	19.30
Ores	100.00	100.00	0.37	0.38	100.00	100.00

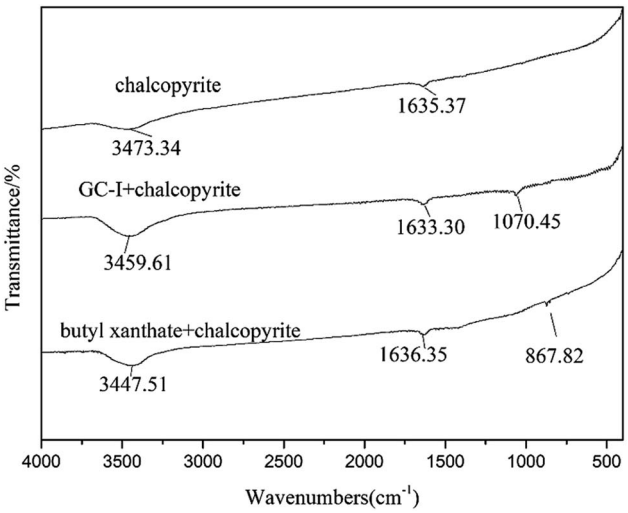

Fig. 8 FTIR spectra of chalcopyrite before and after interaction with collectors.

The monomineral test and actual ore flotation test showed that GC-I had good flotation performance, and its selectivity and collection performance were better than butyl xanthate. In order to further explore the mechanism of GC-I and butyl xanthate, the changes of infrared spectrum of mineral surface before and after the action of agents were analyzed. The infrared spectrum of chalcopyrite and pyrite before and after interaction with GC-I and butyl xanthate were shown in Fig. 8 and 9.

As shown in Fig. 8, after the interaction of GC-I and chalcopyrite, new absorption peaks appeared at 1070.45 cm^{-1}, indicating that new substances were formed on the surface of chalcopyrite by GC-I. Compared with the infrared spectrum of GC-I in Fig. 3, the absorption peak at 1070.45 cm^{-1} was C=S asymmetric stretching vibration absorption peak.[25] After

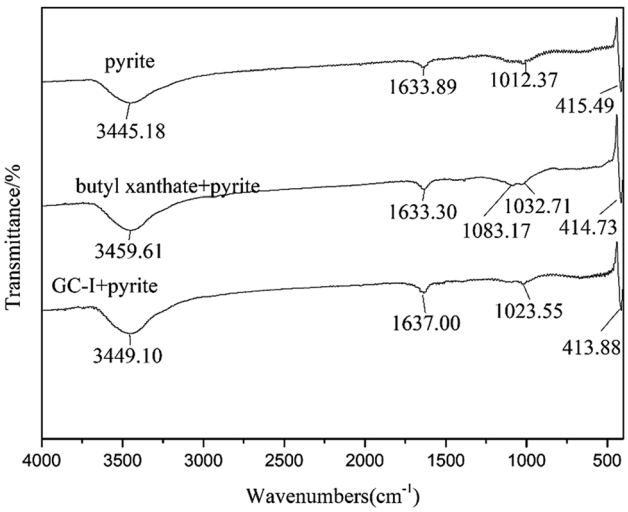

Fig. 9 FTIR spectra of pyrite before and after interaction with collectors.

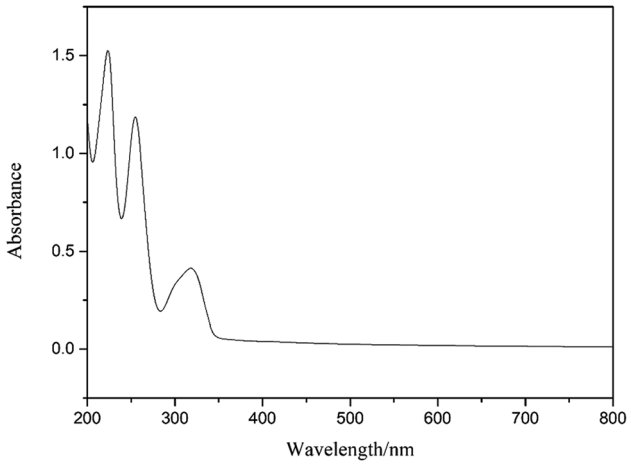

Fig. 10 GC-I ultraviolet spectrum.

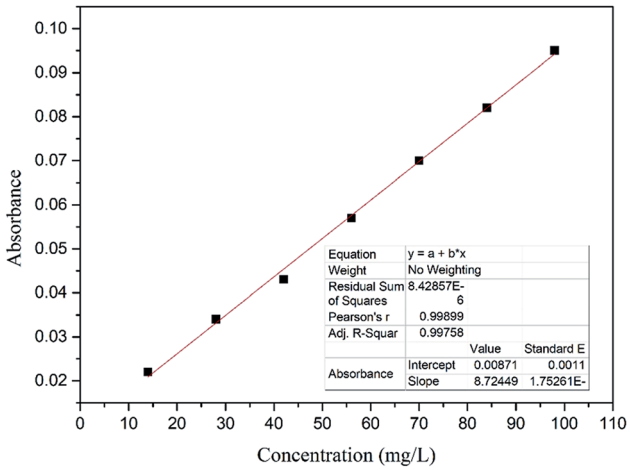

Fig. 11 GC-I adsorption standard curve.

interaction with GC-I, the absorption peak at 3459.61 cm^{-1} was obviously strengthened, which proved that chemical adsorption of GC-I occurred on the surface of chalcopyrite. After the interaction of butyl xanthate and chalcopyrite, a weaker peaks appeared at 867.82 cm^{-1} was due to C–O stretching were prominent.[26] The absorption peak at 3447.51 cm^{-1} was obviously strengthened, which proved that chemical adsorption of butyl xanthate occurred on the surface of chalcopyrite.

As shown in Fig. 9, after the interaction of butyl xanthate and pyrite, new absorption peaks appeared at 1083.17 cm^{-1} and 1032.71 cm^{-1}, the absorption peak at 1083.17 cm^{-1} and 1032.71 cm^{-1} was the valence oscillations of the C=S band,[25] which proved that chemical adsorption of butyl xanthate occurred on the surface of pyrite. However, there was no obvious peak change before and after the interaction of GC-I and pyrite, indicating that physical adsorption between GC-I and pyrite occurred.

In conclusion, chemical adsorption of butyl xanthate occurred on the surface of chalcopyrite and pyrite, chemical adsorption of GC-I occurred on the surface of chalcopyrite, and physical adsorption between GC-I and pyrite occurred, which proved that compared with butyl xanthate, GC-I had stronger selectivity. The separation of copper and sulfur can be achieved by GC-I, which further verifies the results of monominerals flotation.

3.5 Adsorption amount measurement results

The synthesized GC-I was purified by silicon column chromatography and configured into the standard solution of 20 mg L^{-1} GC-I. The ultraviolet spectrum of GC-I was measured, and the adsorption standard curve of GC-I was obtained after diluting the standard solution. The ultraviolet spectrum and adsorption standard curves of GC-I were shown in Fig. 10 and 11. It can be seen from Fig. 11 that $R^2 = 0.99$ from the fitting of the measured standard curve indicated that the concentration of GC-I was linearly related to the adsorption capacity.

In order to further study the adsorption of GC-I on the surface of chalcopyrite and pyrite, the adsorption quantity of GC-I on the surface of minerals was determined under different pH conditions. The test results were shown in Fig. 12.

The variation curves of adsorption quantity of GC-I on the surface of chalcopyrite and pyrite with pH were shown in Fig. 12. With the increase of pH, the adsorption quantity of GC-I on the surface of chalcopyrite increased first. When pH reached 7, the adsorption quantity of GC-I on chalcopyrite surface reached the maximum. After that, with the increase of pH again, the adsorption quantity of GC-I on the surface of chalcopyrite decreased gradually. With the increase of pH, the adsorption quantity of GC-I on the surface of pyrite decreased gradually. The variation trend of the adsorption quantity of GC-I on the surface of chalcopyrite and pyrite was consistent with the monominerals flotation test. As shown in Fig. 12, the optimum pH for interaction between GC-I and chalcopyrite was 7. Under this condition, the effect of GC-I on the surface of chalcopyrite was the most obvious, and the flotation recovery of copper was the highest. According to the adsorption capacity test, when the pulp pH was 7, the adsorption capacity of GC-I on the surface of

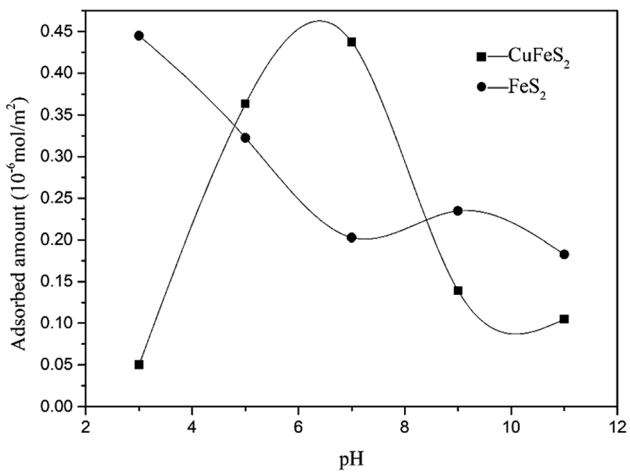

Fig. 12 Variation curves of adsorption quantity of GC-I on the surface of chalcopyrite and pyrite with pH.

chalcopyrite was much higher than that on the surface of pyrite, which proves that GC-I has strong selectivity.

4. Conclusions

Based on the homology principle of higher pharmaceutical chemistry, a new collector for copper sulfide was designed. MS (Materials Studio) was used for molecular dynamics simulation and crystal structure optimization. DFT was used to calculate the interaction energy between reagents and mineral surface. A new copper sulfide collector GC-I (*O*-butyl *S*-(1-chloroethyl)carbonodithioate) was finally synthesized. The results of infrared spectrum analysis showed that there were chemical adsorption of GC-I occurred on the surface of chalcopyrite, and however, physical adsorption between GC-I and pyrite occurred. Through the flotation test of pure minerals and actual ores, it was verified that the new collector GC-I of sulfide ores is superior to butyl xanthate in selectivity and collecting ability, and is more suitable for flotation of the complex and refractory copper sulfide with low grade and fine dissemination.

Author contributions

Xiaopeng Chi and Yunshan Guo conceived and designed the experiments; Yunshan Guo and Guoyao Li preformed the experiments; Xiaopeng Chi and Yunshan Guo analyzed the data; Shuiping Zhong and Xulong Lv provided some reagents and experimental materials; Xiaopeng Chi and Yunshan Guo wrote the paper.

Funding

This work was supported by the National Natural Science Foundation of China [grant number 51874101], Opening Foundation of State Key Laboratory of Comprehensive Utilization of Low-Grade Refractory Gold Ores (Zijin Mining Group Co.,Ltd) and the Industry-University-Research Project in Fujian Province, P. R. China [grant number 2017H6010].

Conflicts of interest

The authors declare no conflict interest.

Acknowledgements

The authors would like to thank Testing Center of Fuzhou University for testing support.

References

1 P. Dhar, M. Thornhill and H. Kota, Investigation of copper recovery from a new copper ore deposit (nussir) in northern norway: dithiophosphates and xanthate-dithiophosphate blend as collectors, *Minerals*, 2019, **9**(3), 380–389.
2 S. A. Khoso, Z. Gao, X. Meng, Y. Hu and W. Sun, The depression and adsorption mechanism of polyglutamic acid on chalcopyrite and pyrrhotite flotation systems, *Minerals*, 2019, **9**(9), 510.
3 A. B. Glembotsky and S. S. Han, Search and "design" for flotation reagents with known properties, *Met. Ore Dress. Abroad*, 1973, (10), 39–41.
4 E. J. Ariens, *Drug design*, Academic Press, 1970, pp. 78–89.
5 B. X. Jian, The structure and regularity of flotation reagent molecules——survey of flotation reagent molecular design with the principles of pharmaceutical chemistry, *Nonferrous Met.*, 1983, (1), 48–57.
6 D. Z. Wang, *Mineral processing and molecular design of metallurgical agents*, Central-South Industry University, Chang sha, 1996, vol. 12, p. 271.
7 Y. R. Jiang, Y. L. Xue and D. Z. Wang, Energy criterion calculation of flotation reagent performance, *J. Cent. South Univ. (Sci. Technol.)*, 1999, (5), 481–484.
8 M. A. M. Abdalla, H. Peng, D. Wu, L. Abusin and T. J. Mbah, Prediction of hydrophobic reagent for flotation process using molecular modeling, *ACS Omega*, 2018, **3**(6), 6483–6496.
9 V. Jain, Pradip and B. Rai, Density functional theory computations for design of salicylaldoxime derivatives as selective reagents in solvent extraction of copper, *Trans. Indian Inst. Met.*, 2016, **69**(1), 135–141.
10 G. Liu, J. Xiao, D. Zhou, H. Zhong, P. Choi and Z. Xu, A DFT study on the structure–reactivity relationship of thiophosphorus acids as flotation collectors with sulfide minerals: implication of surface adsorption, *Colloid. Surf. Physicochem. Eng. Asp.*, 2013, **434**, 243–252.
11 A. Otero-Calvi, L. A. Montero and W.-D. Stohrer, DFT modelling of cobalt and nickel complexes with dithiophosphinic acid, *J. Mol. Struct.: THEOCHEM*, 2008, **859**(1–3), 93–97.
12 M. Q. Jiang, *Advanced pharmaceutical chemistry*, Science Press, Beijin, 1958, p. 05.
13 R. Belissont, M. Munoz, M.-C. Boiron, B. Luais and O. Mathon, Germanium crystal chemistry in cu-bearing sulfides from micro-xrf mapping and micro-xanes spectroscopy, *Minerals*, 2019, **9**(4), 227.
14 H. B. Zhao, Y. S. Zhang, M. L. Sun, P. F. Ou, Y. J. Zhang, R. Liao, *et al.*, Catalytic mechanism of silver in the oxidative dissolution process of chalcopyrite: experiment and dft calculation, *Hydrometallurgy*, 2019, **187**, 18–29.
15 M. V. Gapanovich, I. N. Odin, E. V. Rabenok, P. S. Orishina and G. F. Novikov, Defect structure and photogenerated carrier loss processes in $cu_{1-x}(In_{0.7}ga_{0.3})se_2$ ($0 <= x <= 0.30$) chalcopyrite solid solutions, *Inorg. Mater.*, 2019, **55**(7), 648–652.
16 X. Qi, H. J. Zhang, Y. Q. Li and J. H. Chen, Density functional theory study of the structure and properties of c-doped pyrite, *Phys. B*, 2019, **572**, 168–174.
17 Y. H. Hu, Z. Y. Gao, W. Sun and X. W. Liu, Anisotropic surface energies and adsorption behaviors of scheelite crystal, *Colloid. Surf. Physicochem. Eng. Asp.*, 2012, **415**, 439–448.
18 Pradip, B. Rai, T. K. Rao, S. Krishnamurthy, R. Vetrivel, J. Mielczarski, *et al.*, Molecular modeling of interactions of

diphosphonic acid based surfactants with calcium minerals, *Langmuir*, 2002, **18**(3), 932–940.

19 B. Rai, P. Sathish, J. Tanwar, Pradip, K. S. Moon and D. W. Fuerstenau, A molecular dynamics study of the interaction of oleate and dodecylammonium chloride surfactants with complex aluminosilicate minerals, *J. Colloid Interface Sci.*, 2011, **362**(2), 510–516.

20 L. Y. Dong, H. L. Zhu, F. Jiao, W. Q. Qin and W. H. Jia, Effect of calcium ions on scheelite flotation using mixed collectors, *Sep. Sci. Technol.*, 2019, **54**(1), 153–162.

21 S. A. Khoso, Y. H. Hu, F. Lyu, R. Q. Liu and W. Sun, Selective separation of chalcopyrite from pyrite with a novel non-hazardous biodegradable depressant, *J. Clean. Prod.*, 2019, **232**, 888–897.

22 D. Z. Wei, *Solid material separation*, Metallurgical Industry Press, Beijing, 2009, pp. 88–92.

23 X. j. Sun, G. H. Gu, J. H. Li and Y. H. Hu, Influences of collector CSU31 on chalcopyrite and pyrite flotation, *J. Cent. South Univ. (Sci. Technol.)*, 2010, **41**(02), 406–410.

24 L. Wang, Y. B. Li and W. Q. Li, Influencing mechanism of ions with different valences on chalcopyrite flotation, *Metal. Mine*, 2018, (12), 84–88.

25 E. V. Koporulina, M. V. Ryazantseva, E. L. Chanturiya and E. S. Zhuravleva, Butyl-xanthate adsorption on the surface of sulfide minerals under conditions of their preliminary treatment with water electrolysis products according to atomic-force microscopy and infrared Fourier spectroscopy data, *J. Surf. Invest.: X-Ray, Synchrotron Neutron Tech.*, 2018, **12**(5), 877–886.

26 A. J. Vreugdenhil, S. H. R. Brienne, I. S. Butler, J. A. Finch and R. D. Markwell, Infrared spectroscopic determination of the gas-phase thermal decomposition products of metal-ethyldithiocarbonate complexes, *Spectrochim. Acta A Mol. Biomol. Spectrosc.*, 1997, **53**(12), 2139–2151.

